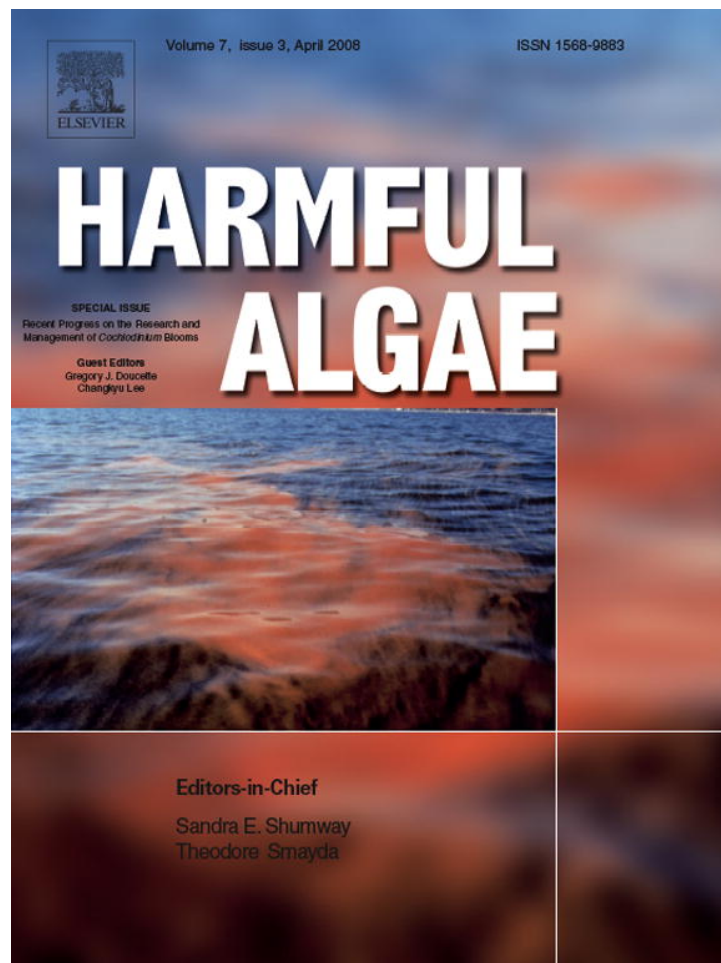


Provided for non-commercial research and education use.
Not for reproduction, distribution or commercial use.



This article was published in an Elsevier journal. The attached copy is furnished to the author for non-commercial research and education use, including for instruction at the author's institution, sharing with colleagues and providing to institution administration.

Other uses, including reproduction and distribution, or selling or licensing copies, or posting to personal, institutional or third party websites are prohibited.

In most cases authors are permitted to post their version of the article (e.g. in Word or Tex form) to their personal website or institutional repository. Authors requiring further information regarding Elsevier's archiving and manuscript policies are encouraged to visit:

<http://www.elsevier.com/copyright>



Characterization, dynamics, and ecological impacts of harmful *Cochlodinium polykrikoides* blooms on eastern Long Island, NY, USA

Christopher J. Gobler^{a,*}, Dianna L. Berry^a, O. Roger Anderson^b, Amanda Burson^a, Florian Koch^a, Brooke S. Rodgers^a, Lindsay K. Moore^a, Jennifer A. Goleski^a, Bassem Allam^a, Paul Bowser^c, Yingzhong Tang^a, Robert Nuzzi^d

^a School of Marine and Atmospheric Sciences, Stony Brook University, Stony Brook, NY 11794-5000, USA

^b Biology, Lamont-Doherty Earth Observatory of Columbia University, 61 Route 9W, Palisades, NY 10964, USA

^c Aquatic Animal Health Program, Department of Microbiology and Immunology, College of Veterinary Medicine, Cornell University Ithaca, NY 14853-6401, USA

^d Suffolk County Department of Health Services, Office of Ecology, Yaphank, NY 11980, USA

Received 16 November 2006; received in revised form 1 February 2007

Abstract

We report on the emergence of *Cochlodinium polykrikoides* blooms in the Peconic Estuary and Shinnecock Bay, NY, USA, during 2002–2006. Blooms occurred during late summer when temperatures and salinities ranged from 20 to 25 °C and 22 to 30 ppt, respectively. Bloom patches achieved cell densities exceeding 10^5 ml⁻¹ and chlorophyll *a* levels exceeding 100 μg l⁻¹, while background bloom densities were typically 10^3 – 10^4 cells ml⁻¹. Light, scanning electron and ultrathin-section transmission electron microscopy suggested that cells isolated from blooms displayed characteristics of *C. polykrikoides* and provide the first clear documentation of the fine structure for this species. Sequencing of a hypervariable region of the large subunit rDNA confirmed this finding, displaying 100% similarity to other North American *C. polykrikoides* strains, but a lower similarity to strains from Southeast Asia (88–90%). Bioassay experiments demonstrated that 24 h exposure to bloom waters ($>5 \times 10^4$ cells ml⁻¹) killed 100% of multiple fish species (1-week-old *Cyprinodon variegatus*, adult *Fundulus majalis*, adult *Menidia menidia*) and 80% of adult *Fundulus heteroclitus*. Microscopic evaluation of the gills of moribund fish revealed epithelial proliferation with focal areas of fusion of gill lamellae, suggesting impairment of gill function (e.g. respiration, nitrogen excretion, ion balance). Lower fish mortality was observed at intermediate *C. polykrikoides* densities (10^3 – 10^4 cells ml⁻¹), while fish survived for 48 h at cell densities below 1×10^3 cells ml⁻¹. The inability of frozen and thawed-, or filtered (0.2 μm)-bloom water to cause fish mortality suggested that the thick polysaccharide layer associated with cell membranes and/or a toxin principle within this layer may be responsible for fish mortality. Juvenile bay scallops (*Argopecten irradians*) and American oysters (*Crassostrea virginica*) experienced elevated mortality compared to control treatments during a 9-day exposure to bloom water ($\sim 5 \times 10^4$ cells ml⁻¹). Surviving scallops exposed to bloom water also experienced significantly reduced growth rates. Moribund shellfish displayed hyperplasia, hemorrhaging, squamation, and apoptosis in gill and digestive tissues with gill inflammation specifically associated with areas containing *C. polykrikoides* cells. In summary, our results indicate *C. polykrikoides* blooms have become annual events on eastern Long Island and that bloom waters are capable of causing rapid mortality in multiple species of finfish and shellfish.

© 2007 Elsevier B.V. All rights reserved.

Keywords: *Cochlodinium*; Fish kill; Harmful algal blooms; Histopathology; Long Island; Peconic Estuary; Polysaccharides; Red tide; Shellfish; TEM and SEM fine structure; Toxicity

1. Introduction

Harmful algal blooms (HABs) represent a significant threat to fisheries, public health, and economies around the world and

have increased in frequency, duration, and distribution in recent decades. HABs are most commonly caused by dinoflagellates which, under bloom conditions, can discolor effected waters red and thus have also been deemed red tides, particularly in Southeast Asia (Okaichi, 2003). Many harmful dinoflagellates synthesize potent biotoxins which can poison humans when shellfish which have concentrated such toxic cells are consumed. However, these toxins often do not harm marine

* Corresponding author. Tel.: +1 631 632 5043; fax: +1 631 632 5070.

E-mail address: christopher.gobler@stonybrook.edu (C.J. Gobler).

life (Landsberg, 2002). Other dinoflagellates can cause direct harm to or even kill marine animals, such as fish, although the precise modes of impairment to the animals are diverse and sometimes not known. One dinoflagellate which is well known for causing fish kills in Southeast Asian waters is *Cochlodinium polykrikoides*.

Cochlodinium has been implicated in kills of wild and impounded fish around the globe (Onoue et al., 1985; Yuki and Yoshimatsu, 1989; Guzmán et al., 1990; Qi et al., 1993; Gárrate-Lizárraga et al., 2004; Whyte et al., 2001) and has been the cause of fisheries losses exceeding \$100 million in Korea (Kim, 1998; Kim et al., 1999). Studies have also indicated that metamorphosis of oyster (*Crassostrea gigas*) larvae was slowed during *Cochlodinium* blooms (Matsuyama et al., 2001) and that mortality of larvae of the American oyster, *Crassostrea virginica*, was elevated by exposure to *Cochlodinium* (Ho and Zubkoff, 1979). The most common *Cochlodinium* species, *C. polykrikoides*, grows optimally at temperatures between 21 and 26 °C and at salinities between 30 and 36 (Kim et al., 2004; Yamatogi et al., 2006). *Cochlodinium* is a mixotrophic alga (Larsen and Sournia, 1991; Jeong et al., 2004) and thus likely employs flexible nutrient acquisition strategies during blooms. Moreover, since this alga is noxious to some planktonic grazers (Ho and Zubkoff, 1979; Shin et al., 2003), it may escape top-down control by zooplankton which most phytoplankton experience (e.g. Gobler et al., 2002). Prior to this special issue, peer-reviewed reports of *Cochlodinium* blooms in the US have been rare and blooms in NY waters have never been noted in peer-reviewed literature.

The occurrence of HABs in Long Island estuaries has been well documented for more than 50 years. During the 1950s, Ryther (1954) described the occurrence of green tide blooms caused by the chlorophytes *Nannochloris* and *Stichococcus* in the south shore estuaries, Great South Bay and Moriches Bay. These blooms negatively impacted the oyster fishery in these systems (Ryther, 1989). More recently, brown tides caused by the pelagophyte *Aureococcus anophagefferens* occurred in both south shore bays (Great South, Moriches, and Shinnecock Bays) and on eastern Long Island (Peconic Estuary; Gobler

et al., 2005). Chronic recurrence of these blooms in the Peconic Estuary for 10 years and on the south shore for more than 15 years led to the destruction of eel grass beds (*Zostera marina*), scallop fisheries (*Argopecten irradians*), and hard clam fisheries (*Mercenaria mercenaria*; Gobler et al., 2005). The absence of brown tides on Long Island in recent years has buttressed hope that local fisheries may recover.

Here, we report on the emergence and dynamics of red tides caused by *Cochlodinium polykrikoides* in some of the same estuaries which formerly hosted brown tides, the Peconic Estuary and Shinnecock Bay. We describe the initial occurrence of blooms in 2002 and 2004, and the spatial and temporal dynamics of blooms in 2005 and 2006. We present light, scanning and thin-section transmission electron micrographs of algal isolates, as well as sequences of the large subunit ribosomal DNA. We describe the results of experiments with multiple species of finfish and shellfish to elucidate the potential for blooms to impact marine life in these systems and present histopathological analysis of moribund individuals. Finally, we analyze current and historical water quality data to assess possible bloom causes and to compare and contrast these blooms to those of the brown tide, *A. anophagefferens*.

2. Methods

2.1. Field sampling and sample processing

Fixed stations within the Peconic Estuary and Shinnecock Bay and their respective tributaries (Fig. 1) were sampled via small research vessels sporadically in 2004 and 2005 and weekly to biweekly during the summer of 2006. Moreover, in 2006, bloom patches were sampled in addition to fixed stations. Primary stations in 2006 included the two most western basins of the Peconic Estuary, Flanders Bay (40.923°N, 72.587°W) and Great Peconic Bay (40.936°N, 72.512°W), as well as Meetinghouse Creek (40.938°N, 72.619°W), a tributary which empties into Flanders Bay, and Old Fort Pond (40.868°N, 72.446°W), a tidal tributary in eastern Shinnecock Bay. On station, temperature and salinity were determined using a

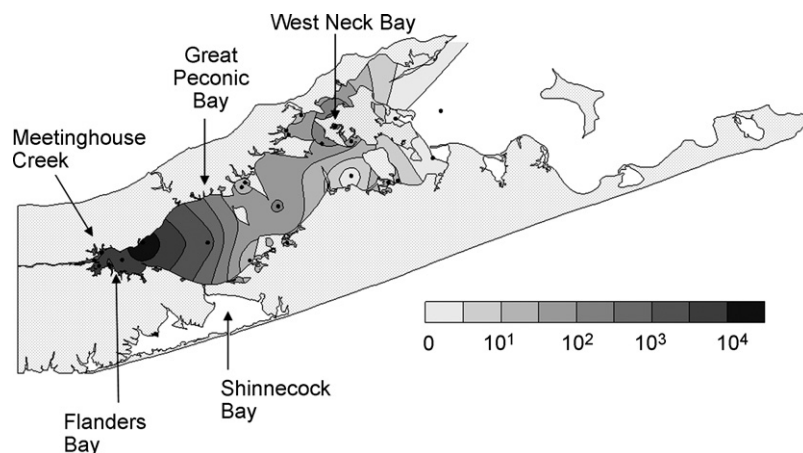


Fig. 1. Spatial distribution of *Cochlodinium* cells in the Peconic Estuary, early September 2005. Gradients are based log of cell densities measured at 25 locations across the estuary.

Hydrolab Quanta probe. Surface water samples at each station were collected from the bow of boats in replicated 20 l carboys which were transported to the Stony Brook-Southampton Marine Science Center for immediate sample processing and analysis.

2.2. Quantification of chlorophyll *a* (*chl a*) and cell densities in field samples

Triplicate chlorophyll *a* samples were collected on GF/F glass fiber filters and stored frozen. Chlorophyll *a* was size-fractionated using a 5 µm Nitex[®] mesh. Whole seawater samples were preserved in Lugol's iodine for microscopic examination of phytoplankton. Chlorophyll *a* was analyzed in triplicate by standard fluorometric methods (Parsons et al., 1984). Preserved plankton samples were settled in counting chambers and enumerated on an inverted light microscope (Hasle, 1978). At least 100 cells were enumerated per sample, yielding a relative standard deviation of less than 20% for *Cochlodinium* enumeration at bloom and non-bloom densities. The relative abundance of *Cochlodinium* among autotrophs in selected samples was estimated from lengths and widths of the most common phytoplankton present and using volumetric equations corresponding to the geometric shape each organism most resembled (Smayda, 1978; Stoecker et al., 1994).

2.3. Culture establishment, DNA analysis, and morphological observations with light microscope (LM), scanning electron microscopic (SEM) and transmission electron microscope (TEM)

Culture isolates were obtained by pipetting single cells to polystyrene 12-well cell culture plates containing culture medium under an inverted microscope. Cells were cultured in sterile *f*/20 medium supplemented with 10⁻⁸ M selenium at 22 °C in an incubator with a 14 h light:10 h dark cycle, illuminated by a bank of fluorescent lights that provided a light intensity of ~100 µmol quanta m⁻² s⁻¹ to cultures. Cultures were transferred once they reached stationary phase which was approximately 3 weeks. Light microscope photographs were obtained using an inverted microscope and a Spot Insight (model 3.2) camera.

For genetic analysis, cells were pelleted by centrifugation of 3 ml of culture at 5 K rpm for 2 min. The cell pellet was immediately resuspended in 600 µl CTAB solution (100 mM Tris-HCl [pH 8], 1.4 M NaCl, 20 mM EDTA, 2% [w/v] cetyltrimethylammonium bromide [CTAB], 0.4% [v/v] β-mercaptoethanol, 1% [w/v] polyvinylpyrrolidone; Dempster et al., 1999) and cells were disrupted by vortexing and pipetting. The resuspended cells were frozen at -80 °C for at least 1 h. Nucleic acids were extracted as in Coyne et al. (2001). The hypervariable D1–D3 region of the rDNA was amplified by PCR using forward primer 'D1RF' (5'-ACCCGCTGAATT-TAAGCATA-3') and reverse primer 'D3Car' (5'-ACGAAC-GATTTGCACGTCAG-3'; Mikulski et al., 2005). The D4–D6 region was amplified with forward primer 6F (5'-TAG-TAGCTGGTTCCCTCCGA-3') and reverse primer 11R (5'-

TTGCCGACTTCCCTTACCTA-3'; Iwataki et al., 2008). PCR was performed with the following components: 80–100 ng nucleic acids, 0.5 µM of each primer, 1× reaction buffer, 3 mM MgCl₂, 200 µM dNTPs mix (New England Biolabs), 0.5 µM of each primer, 2.5 U polymerase enzyme mix (GeneAmp[®] High Fidelity PCR Applied Biosystems). We performed 50 µl reactions with the following cycling parameters: 94 °C for 5 min, followed by 31 cycles of 94 °C for 45 s, 45 °C for 60 s and 72 °C for 45 s, followed by 72 °C final extensions for 7 min (Mikulski et al., 2005). Sequencing was done directly on the unmodified PCR product using 50 ng of PCR product and 3.2 pmol primer on a ABI3730 Genetic Analyzer using BigDye Terminator[®] Cycle sequencing kit (Applied Biosystems) at the Stony Brook University DNA Sequencing Facility.

To preserve field samples for electron microscopy, equal volumes of buffered glutaraldehyde fixative and algal suspension from the sampling site were mixed to produce a final solution of 2% glutaraldehyde in 0.05 M cacodylate buffered seawater (pH 8.0) at 5 °C. The fixed cells were gently sedimented to form a pellet, the supernatant was decanted, and 5 ml of 4% osmium tetroxide solution in the same cacodylate buffer was added to the pellet as a post stain and fixative. After 1 h at 5 °C, the osmium-fixed cells were sedimented, washed by addition of cacodylate buffer and again sedimented to form a pellet and enrobed in 0.8% agar matrix. Small segments of the agar-embedded pellet (~3 mm in size) were washed in deionized water, dehydrated in a graded acetone/aqueous series, embedded in TAAB epoxy resin (Energy Beam Sciences, Granby, Conn.) and polymerized in BEEM capsules at 70 °C for 18 h. Ultrathin sections, collected on uncoated copper grids, were obtained with a Porter-Blum MT-2 ultramicrotome fitted with a diamond knife, post-stained with Reynold's lead citrate, and observed with a Philips 201 transmission electron microscope. A portion of the osmium-fixed cells was set aside for scanning electron microscopic observation. The fixed cells were sedimented, washed with deionized water, and brought to a volume of 2 ml in 10% ethanol solution. Cells were collected on 0.45 µm pore-size Millipore nitrocellulose filters, dehydrated in a graded ethanol/aqueous series, and critical point dried using a Balzer critical point dryer. The dried filters were attached to SEM stubs, plated with gold using a Denton Desktop 2 sputter coater, and observed with a LEO 1455VP scanning electron microscope. Higher resolution images of cell surface detail were obtained with a Hitachi 4700 SEM.

2.4. Bioassay experiments

Experiments were conducted to elucidate the potential impact of *Cochlodinium* sp. bloom water on fish and shellfish. One set of experiments was performed with juvenile (1–3-week-old) sheepshead minnows (*Cyprinodon variegates*) spawned from a line of *C. variegates* which has been laboratory reared for more than a decade (E.M. Cospes, personal communication). For these experiments, individual minnows were transferred using a modified 200 µl pipette to 3 ml of treatment water held in 24-well sterile, polystyrene plates

($n = 24$ per treatment). In the first experiment, *C. variegates* were transferred to plates containing one of four treatment waters: (1) bloom water from Flanders Bay (Fig. 1) containing 5×10^4 cells ml^{-1} , (2) filtered bloom water (0.2 μm), (3) water from Great Peconic Bay (Fig. 1), which had $<1 \times 10^2$ cells ml^{-1} , or (4) filtered (0.2 μm) Great Peconic Bay water. Subsequent experiments were conducted using 100% bloom water from Flanders Bay or Old Fort Pond (Fig. 1), as well as bloom water diluted with 0.2 μm -filtered bloom water to final concentrations of bloom water of 50, 25, 10, and 0% to elucidate a dose response. To further understand modes of mortality, experiments were conducted using boiled or frozen and thawed bloom water as treatments, as well as water which was passed through 2.0 μm polycarbonate filters, a 10 μm nylon mesh or a 20 μm nylon mesh. In all experiments, control treatments of non-bloom Great Peconic Bay water and/or filtered bloom water (0.2 μm) were established which yielded 100% survival for the full duration of all experiments (72 h). Fish in experiments were checked several times daily and dead individuals were immediately removed and placed in 10% neutral buffered formalin for later histopathological evaluation.

Larger fish for experiments (*Fundulus majalis*, *Fundulus heteroclitus*, *Menidia menidia*) were obtained via seine nets from regions of Shinnecock Bay with undetectable levels of *Cochlodinium* sp. Fish were maintained in aerated seawater with low levels of *Cochlodinium* sp. at the Stony Brook-Southampton Marine Science Center for 24 h prior to experiments. Experiments were established by placing 10 individuals in triplicate 5-l plastic containers holding 3 l of bloom water from Flanders Bay or Eastern Shinnecock Bay ($>10^4$ cells ml^{-1}) or water from Great Peconic Bay (Fig. 1) which had $<1 \times 10^2$ cells ml^{-1} . All containers were placed in flow through seawater to maintain ambient temperature and were bubbled with air, maintaining oxygen levels above 5 mg l^{-1} . Containers were covered with white, nylon screening with 1 mm mesh openings. Dilutions of bloom water with filtered (0.2 μm) bloom water (50, 25, 10%) were created for experiments with *F. majalis* and *M. menidia* to elucidate a dose response in the fish. Fish survival was examined every 1–8 h and dead fish were immediately removed and placed in 10% neutral buffered formalin for later histopathological evaluation. Experiments with *F. majalis*, *F. heteroclitus*, and *M. menidia* lasted 24–48 h. Spectrophotometrically analyzed ammonium levels (Parsons et al., 1984) remained $<20 \mu\text{M}$ during fish experiments.

A. irradians and *C. virginica* bioassay experiments were conducted using juvenile bay scallops (~11 mm) and American oysters (~21 mm) obtained from the Cornell Cooperative Extension shellfish hatchery facility in Southold, NY. Shellfish were maintained in flowing seawater at the Stony Brook-Southampton Marine Science Center for 24 h prior to experiments. Experiments were established by measuring the lengths of 10 marked individuals and placing them in triplicate, 5-l plastic buckets (10 individuals per bucket) containing 3 l of: (1) bloom water from Flanders Bay (Fig. 1) containing $\sim 5 \times 10^4$ cells ml^{-1} , (2) filtered (0.2 μm) treatment #1 water

(Flanders Bay), (3) water from Great Peconic Bay (Fig. 1), which had $<1 \times 10^2$ cells ml^{-1} , or (4) filtered (0.2 μm) treatment #3 water (Great Peconic Bay). All buckets were kept in a temperature-controlled room maintained at 24 °C with light from a bank of fluorescent bulbs which provided 100 $\mu\text{E m}^{-2} \text{s}^{-1}$ of light on a 14 h light:10 h dark cycle. All buckets were bubbled with air, maintaining oxygen levels above 5 mg l^{-1} , and covered with white, nylon screening with 1 mm mesh openings. Experimental water was fully exchanged with newly obtained water from the field with comparable cell numbers every other day during this 9-day experiment. Mean cell densities (\pm S.D.) for the experiment were $3.7 \pm 1.3 \times 10^4$ cells ml^{-1} (range = 2.7–6.1 $\times 10^4$ cells ml^{-1}). Samples for the enumeration of phytoplankton cell densities and chlorophyll *a* levels were obtained from the old and new water and analyzed every other day as described above. Survival was examined daily and dead individuals were immediately measured, shucked and placed in 10% neutral buffered formalin for later histopathological evaluation. After 9 days, lengths of surviving individuals were measured.

Experiments that involved larger fish and scallops were analyzed via one-way ANOVAs followed by Tukey multiple comparisons tests of treatments (Sokal and Rohlf, 1995). Non-normally distributed data sets were log transformed. Experiments using sheepshead minnows were analyzed using Chi-square tests. In all cases, significance levels were set at $p < 0.05$.

2.5. Histopathology

All specimens were fixed in 10% neutral buffered formalin for a minimum of 1 week before being processed for histology using standard techniques. For scallops and oysters, a cross-section of about 6 mm in thickness (typically containing mantle, gills, digestive gland, stomach, intestine, heart and kidney) was transferred to a pre-labeled histo-cassette, and dehydrated in graded ethanol and xylene series. Tissues were then embedded in paraffin and sectioned (5 μm thick). Resulting sections were stained with hematoxylin and eosin, before being examined with a Nikon Eclipse TE-200 microscopy equipped with a Spot Insight QE digital camera. Fish were decalcified with sodium EDTA (Luna, 1968). In the case of the smallest fish (1–3-week-old *C. variegates*), the specimens were sectioned whole in the median plane in three step sections: 1/8-way toward the mid-median plane, 1/2-way toward the mid-median plane and at the mid-median plane. For all other fish, gills were dissected from the fish for processing. Tissues were then embedded in paraffin, sectioned and stained with hematoxylin and eosin stains for histological evaluation (Luna, 1968).

3. Results

3.1. Bloom dynamics

The first noted appearance of *Cochlodinium* on eastern Long Island was in 2002, when it was identified as the organism

responsible for a red water event in West Neck Bay, on Shelter Island (Fig. 1). The first geographically extensive bloom occurred within the Peconic Estuary in September and October of 2004 when cell densities ranging from 1 to $2 \times 10^3 \text{ ml}^{-1}$ were recorded in the two western basins of this system, Flanders Bay and Great Peconic Bay (Fig. 1). A bloom occurred within the same regions in 2005, with station cell densities exceeding 10^3 ml^{-1} in the western Peconic Estuary (Fig. 1) and patch densities exceeding $2 \times 10^4 \text{ cells ml}^{-1}$. In contrast, low cell densities ($<10^4 \text{ ml}^{-1}$) were found in the major basins of the eastern Peconic Estuary, although some tributaries and sub-embayments such as West Neck Bay, had higher densities (Fig. 1).

In 2006, a more robust sampling approach allowed the details of *Cochlodinium* bloom temporal dynamics to be refined. *Cochlodinium* was detected for the first time in the water column in July at all major sampling locations as temperatures were approaching 25°C (Fig. 2; Table 1). *Cochlodinium* maintained moderate cell densities (10^2 – $10^3 \text{ cells ml}^{-1}$) through mid-August as temperatures reached an annual maximum above 25°C at all sites (Fig. 2; Table 1). During the period of 20 August through 21 September, cell densities within four major sampling locations (Flanders Bay, Meetinghouse Creek, Great Peconic Bay, eastern Shinnecock Bay) were consistently $>10^3 \text{ cells ml}^{-1}$ and were commonly $>10^4 \text{ cells ml}^{-1}$ (Fig. 2). Concurrently, chlorophyll *a* levels often exceeded $100 \mu\text{g l}^{-1}$ (range 54–370) with nearly all chlorophyll being $>5 \mu\text{m}$, as temperatures were declining to 20°C (Table 1). During the same period, dense bloom patches were chronically present throughout the four major stations, with patch cell densities ranging between 10^4 and $10^5 \text{ cells ml}^{-1}$ (Fig. 2). By late September, cell densities once again declined to $<10^2 \text{ cells ml}^{-1}$ at all locations as temperatures dropped below 20°C (Fig. 2; Table 1). Salinities at three of four sites generally ranged from 25 to 30 and were highest during the late August bloom peak (Fig. 2; Table 1). Meetinghouse Creek had lower salinities throughout the study (22–25; Table 1).

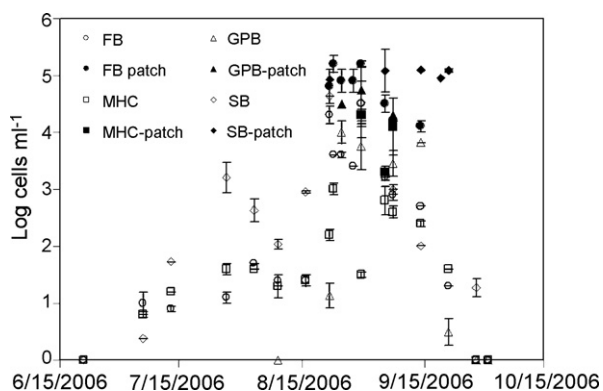


Fig. 2. Log of *Cochlodinium* cell densities recorded during the summer of 2006 in Flanders Bay (FB: circles), Meetinghouse Creek (MHC: squares), Great Peconic Bay (GPB: triangles), and eastern Shinnecock Bay (SB: diamonds). Open symbols represent fixed stations, whereas closed symbols represent dense bloom patches present at each location. Error bars are standard error of triplicate field samples.

3.2. Molecular and microscopic characterization of cells

There were considerable variations in cell sizes of the unpreserved *Cochlodinium* sp. isolates, with an average of $34 \pm 4.7 \mu\text{m}$ long (range 21–35 μm) and $27 \pm 4.1 \mu\text{m}$ wide (range 24–48 μm ; $n = 100$). A LM view of isolated, living cells (Fig. 3) exhibits the major morphological features of paired and catenated cells in a chain. The leading cell in a chain frequently contains a more tapered, semi-circular epicone. The hypocone is bigger than the epicone in both width and length, slightly or heavily bilobbed at the antapex, most easily observed in single cell or the last cell in a chain. The left spiral cingulum is deeply grooved, with about two turns of torsion. The sulcus is narrow, with a torsion of about one turn. Intermediate cells within a chain are slightly compressed longitudinally and thus more rounded to ovate. A reddish stigma is visible in the left side of the apical region of the epicone (Fig. 3). The nucleus is small and located at the center of the epicone (Fig. 3).

A SEM micrograph of a field-collected and possibly stressed four-cell chain displays the extensive exocellular organic fibrillar matrix (Fig. 4A, arrow). More slender tubular extensions from the surface of some cells appear to be discharged trichocysts. A higher magnification of SEM (Fig. 4B) shows the network organization of the secretory fibrils enclosing the cell surface. In addition to the exocellular organic matrix, the cell is surrounded by a more closely enclosing organic envelope (Fig. 4C) that partially obscures the underlying cingulum (thick arrow) and is more clearly evidenced at places where it is partially fractured (thin arrow) revealing the underlying cellular surface. An enlarged view of a terminal cell in a chain (Fig. 4E) exhibits the transverse flagellum (thick arrow) encircling the cell slightly anterior to

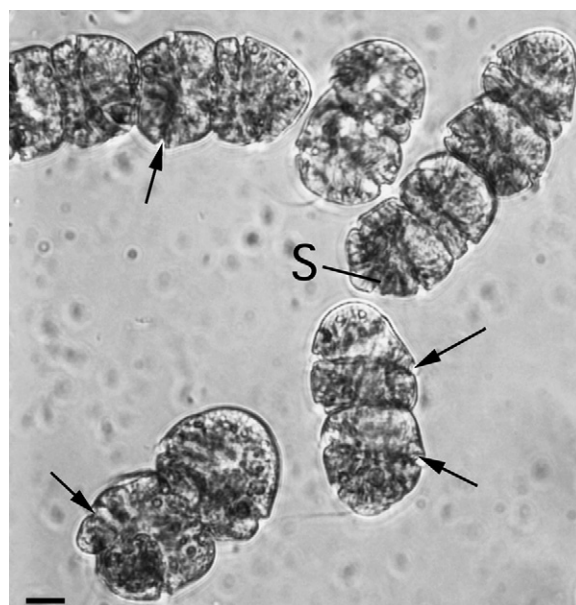


Fig. 3. Light microscopic views of paired and catenated cells of *Cochlodinium* sp. showing the major morphological features, including the somewhat rounded form of the cells, especially those more internal in a chain, and the surface details, e.g. sulcus (S) and the deeply grooved cingulum (arrows). Scale bar = 10 μm .

Table 1
 Temperature (*T*) in °C, salinity (*S*), *Cochlodinium polykrikoides* cell densities from fixed station sampling (cells), and *Cochlodinium polykrikoides* cell densities from bloom patches during August and September (patch) in Flanders Bay, Meetinghouse Creek, Great Peconic Bay, and eastern Shinnecock Bay

| Date | Flanders Bay | | | | Meetinghouse Creek | | | | Great Peconic Bay | | | | Eastern Shinnecock Bay | | | |
|--------------|--------------|----------|-----------|-----------|--------------------|----------|-----------|-----------|-------------------|----------|-----------|-----------|------------------------|----------|-----------|-----------|
| | <i>T</i> | <i>S</i> | Cells | Patch | <i>T</i> | <i>S</i> | Cells | Patch | <i>T</i> | <i>S</i> | Cells | Patch | <i>T</i> | <i>S</i> | Cells | Patch |
| 21-June | 22.5 | 25.6 | 0.0 (0.0) | – | 23.4 | 22.5 | 0.0 (0.0) | – | – | – | – | – | 21.2 | 28.1 | 0.0 (0.0) | – |
| 26-June | 23.0 | 26 | 0.0 (0.0) | – | – | – | – | – | – | – | – | – | – | – | – | – |
| 6-July | 23.9 | 23.7 | 1.0 (0.4) | – | 25.2 | 23.5 | 0.8 (0.1) | – | – | – | – | – | 24.0 | 24.6 | 0.4 (0.0) | – |
| 13-July | 24.6 | 25.9 | 0.9 (0.1) | – | 24.6 | 22.4 | 1.2 (0.0) | – | – | – | – | – | 23.5 | 23.0 | 1.7 (0.0) | – |
| 18-July | 29.1 | 24.4 | 0.7 (0.1) | – | – | – | – | – | – | – | – | – | – | – | – | – |
| 27-July | 26.2 | 26.2 | 1.1 (0.2) | – | 28.3 | 22.1 | 1.6 (0.2) | – | – | – | – | – | 26.2 | 23.6 | 3.2 (0.5) | – |
| 3-August | 29.5 | 25.1 | 1.7 (0.0) | – | 29.1 | 23.5 | 1.6 (0.0) | – | – | – | – | – | 30.8 | 24.9 | 2.6 (0.4) | – |
| 9-August | 27.4 | 26.5 | 1.4 (0.2) | – | 27.7 | 25.5 | 1.3 (0.4) | – | – | – | 0.0 (0.0) | – | 25.1 | 28.3 | 2.0 (0.2) | – |
| 15-August | 25.0 | 25.8 | 1.4 (0.2) | – | 24.6 | 24.3 | 1.4 (0.2) | – | – | – | – | – | 26.3 | 27.3 | 2.9 (0.0) | – |
| 22-August | 25.3 | 26.5 | 4.3 (0.3) | 4.8 (0.6) | 26.5 | 24.9 | 2.2 (0.2) | – | 24.9 | 28.0 | 1.1 (0.4) | – | 25.2 | 28.8 | 1.1 (0.4) | 4.9 (0.4) |
| 23-August | 25.0 | 26.3 | 3.6 (0.0) | 5.2 (0.3) | 24.3 | 23.6 | (0.3) | – | – | – | – | 5.0 (0.4) | – | – | – | – |
| 25-August | 24.0 | 26.1 | 3.6 (0.1) | 4.9 (0.4) | – | – | – | – | 23.5 | 28.5 | 4.0 (0.4) | 4.5 (0.4) | 24.5 | 29 | 4.5 (0.4) | – |
| 28-August | 22.2 | 25.4 | 3.4 (0.0) | 4.9 (0.4) | – | – | – | – | – | – | – | 5.0 (0.3) | – | – | – | – |
| 30-August | 20.6 | – | 4.5 (0.8) | 5.2 (0.1) | 21.1 | 22.2 | 1.5 (0.1) | 4.3 (0.2) | 20.1 | 27.3 | 3.7 (0.8) | 4.7 (0.8) | 20.8 | 29.2 | 1.5 (0.1) | – |
| 5-September | 20.3 | 25.8 | 3.2 (0.1) | 4.5 (0.3) | 20.3 | 24.4 | 2.8 (0.5) | 3.3 (0.2) | 19.9 | 27.3 | – | – | – | – | 5.1 (0.7) | 5.1 (0.1) |
| 7-September | 20.4 | 25.1 | 2.9 (0.2) | 4.2 (0.0) | 20.8 | 23.5 | 2.6 (0.0) | 4.1 (1.0) | 19.9 | 27.5 | 3.5 (0.5) | 4.3 (0.1) | 21.5 | 30.0 | 3.5 (0.5) | – |
| 14-September | 20.1 | 25.3 | 2.7 (0.0) | 4.1 (0.2) | 20.7 | 24.0 | 2.4 (0.1) | – | 19.6 | 27.1 | 3.8 (0.0) | – | 18.6 | 26.8 | 2.4 (0.1) | 5.1 (0.1) |
| 19-September | – | – | – | – | – | – | – | – | – | – | – | – | – | – | 5.0 (0.0) | 5.0 (0.6) |
| 21-September | 19.5 | 25.5 | 1.3 (0.0) | – | 20.1 | 24.7 | 1.6 (0.0) | – | 19.6 | 27.5 | 0.5 (0.4) | – | 55.1 | 27.5 | 1.6 (0.0) | 5.1 (0.1) |
| 28-September | 19.1 | 26.2 | 0.0 (0.0) | – | 19.0 | 22.6 | 0.0 (0.0) | – | 19.2 | 27.4 | 0.0 (0.0) | – | 19.7 | 27.9 | 1.3 (0.3) | – |
| 1-October | 19.0 | 26.1 | 0.0 (0.0) | – | 19.2 | 23.1 | 0.0 (0.0) | – | 19.2 | 27.3 | 0.0 (0.0) | – | 19.4 | 24.7 | 0.0 (0.0) | – |

Cell densities are reported as means and standard deviation on parentheses. Dashes indicate samples from a given location and dates were not obtained.

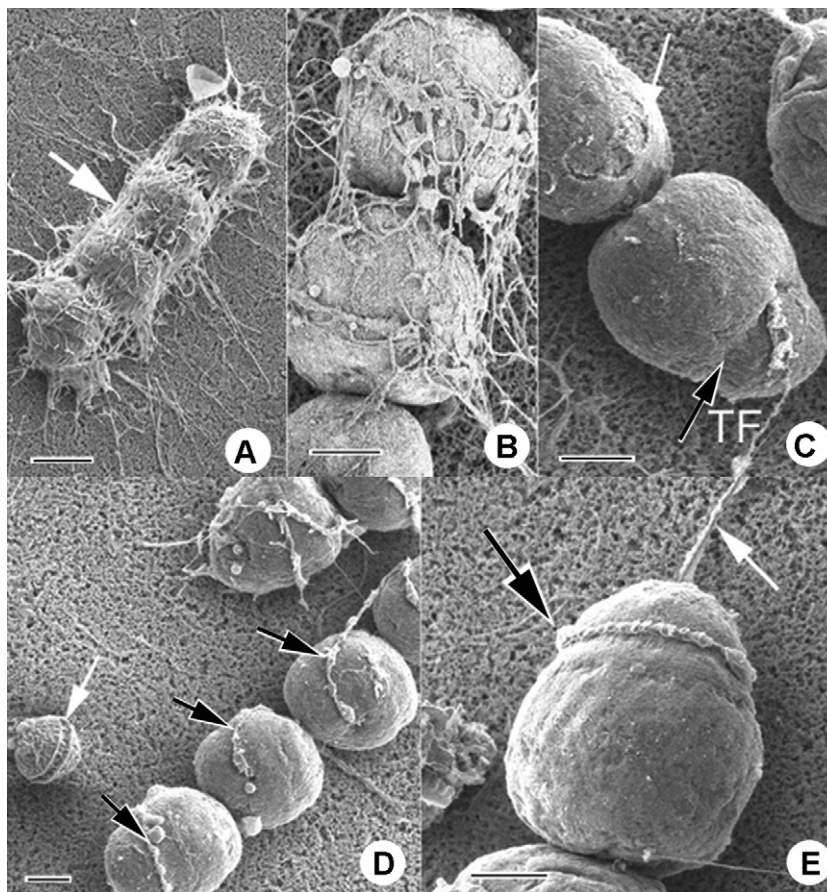


Fig. 4. SEM views of surface details of *Cochlodinium* sp. (A) An overview of four adlined cells with an extensive exocellular fibrillar matrix (arrow) is shown uniting the cells longitudinally and extending outward as filaments anchored to the surface of the Millipore substratum. Scale bar = 20 μm . (B) A higher resolution image of the exocellular matrix showing the fibrillar network in greater detail and the organization of the nodes where the fibrils are joined. Scale bar = 10 μm . (C) An enlarged image of a terminal cell in a chain, and its adjacent neighbor, showing the thin organic envelope or pellicle that encloses each cell and underlies the exocellular fibrillar matrix. The cingulum (black arrow), obscured by the organic envelope and appearing as a surface depression, has an emergent transverse flagellum (TF) that is partially dislocated from the groove and is stretched out across the epicone onto the surrounding Millipore surface. A fracture in the organic envelope (white arrow) reveals the approximate thickness of the envelope and exposes the underlying surface of the cell. Scale bar = 10 μm . (D) A chain of three cells exhibits the transverse flagella (black arrows) in a more typical organization encircling the cell. Note that the middle cell of the three shows a small pore in the organic envelope where the transverse flagellum emerges. For purposes of comparison, an armored, theca-bearing smaller dinoflagellate (white arrow), that was included in the water sample, is shown with a clearly exposed cingulum. Scale bar = 10 μm . (E) An enlarged view of a terminal cell of *Cochlodinium* in a chain, shows the depression of the cingulum in clearer detail, and somewhat anterior to it, the location of the transverse flagellum (black arrow) encircling the epicone. An apparent trailing flagellum (white arrow) extends along the surface of the Millipore filter. Scale bar = 10 μm .

the depression of the cingulum and situated on the surface of the epicone.

An overview of the nuclear region and peripheral cytoplasm (Fig. 5A) as observed by transmission electron microscopy shows the mesocaryotic nucleus (N), approximately 12 μm in diameter, with condensed chromosomes ($\sim 1 \mu\text{m}$ diameter), and some of the large peripheral cytoplasmic vacuoles (V) and plastids (P) that are typically distributed near the periphery of the cytoplasm. The inset (Fig. 5A) illustrates the organization of the two kinds of ejectosomes, elongated trichocyst-like organelles that appear to be quadrangular in cross-section (large arrow) and elongated in longitudinal section (L), and smaller mucocyst ejectosomes (small arrows) that have a dense central core. An enlarged view of the peripheral cytoplasm (Fig. 5B) displays a mitochondrion (arrow) with tubular cristae and, adjacent to it, the peripheral alveolar membranes surrounding the cell with a thin somewhat electron dense

organic deposit within the lumen of the alveolar membranes. A higher magnification image of the cell periphery (Fig. 5C) shows the alveolar membranes (thick arrow) in more detail, including the organic deposit ($\sim 60 \text{ nm}$ thick) within the alveolar space. An organic outer envelope or pellicle, external to the alveolar membranes, is limited externally by an osmiophilic thin layer (thin arrow). This outer layer of the organic envelope lies approximately 1 μm or greater from the plasma membrane and underlying alveolar membranes at the surface of the cell. A thin layer of cytoplasm encloses the cell beneath the organic envelope and immediately external to the alveolar membranes. A segment of a mitochondrion (M) and an ejectosome, that appears to be a mucocyst (E) docked at the plasma membrane, are shown near the peripheral cell membranes. An enlarged view (Fig. 5D) of a typical mitochondrion (M) shows the elongated profile (up to 3 μm long) and the tubular cristae ($\sim 40 \text{ nm}$ in diameter) in greater

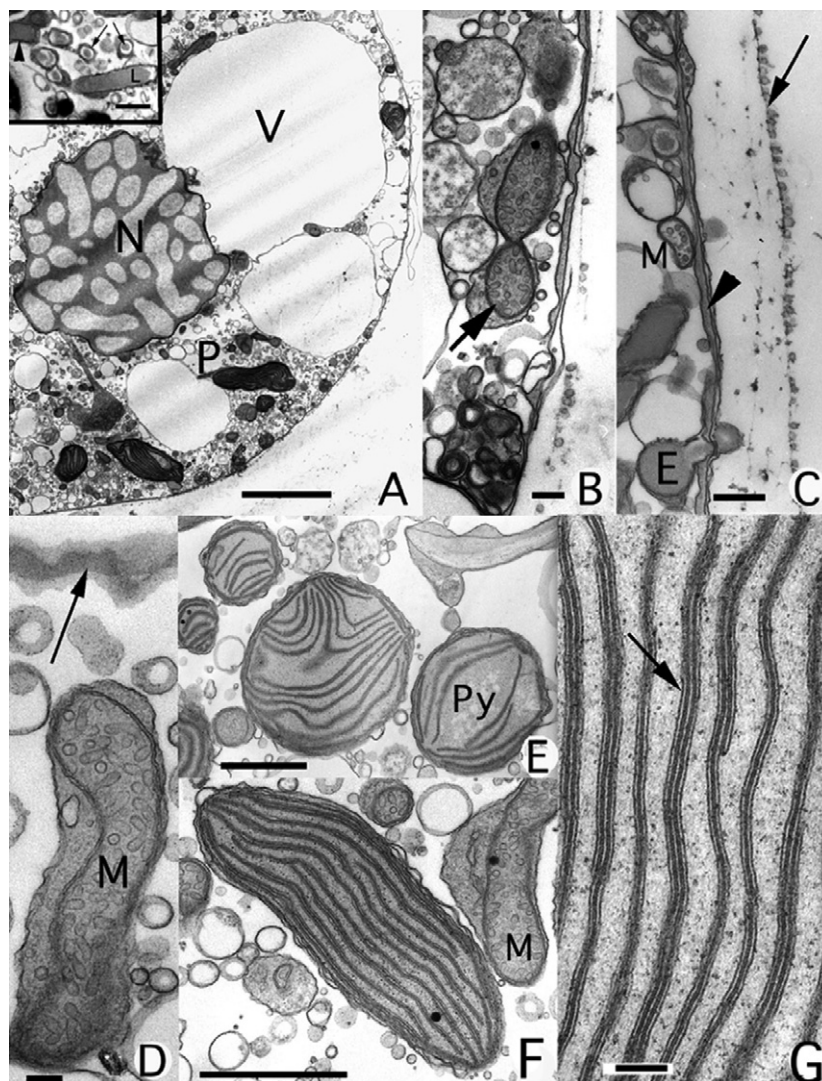


Fig. 5. Transmission electron microscopic images of ultrathin sections of *Cochlodinium* sp. (A) An overview of the nuclear region and peripheral cytoplasm, showing the nucleus (N) located eccentrically near one side of the cell, large vacuoles (V), and chloroplasts (P) near the cell periphery. Scale bar = 5 μm . Inset displays sections of the two kinds of ejectosomes, trichocyst-like organelles that are quadrangular in cross section (large arrow) and elongated in longitudinal section (L), and smaller mucocysts (small arrows) that have a more circular profile in cross section containing an electron dense central core. Compare to the ejectosome (E) in C. Scale bar = 0.5 μm . (B) A higher magnification view of the cell periphery shows a tubulocristate mitochondrion (arrow) within a cytoplasmic lobe near the alveolar membranes at the surface of the cell. Scale bar = 0.2 μm . (C) A high magnification image of the cell surface illustrates the dense organic deposit (arrowhead) within the alveolar lumen and the limiting osmiophilic thin layer (thin arrow) of an organic envelope or pellicle lying external to the cell surface. A thin layer of dense cytoplasm, enclosing the cell and delimited within closely spaced plasma membranes, lies immediately adjacent to the external surface of the alveolar complex. A segment of a mitochondrion (M) and an oblique section through the sac of an ejectosome (E), probably a mucocyst docked at the plasma membrane, are shown within the cytoplasm. Scale bar = 0.4 μm . (D) A high magnification view of a mitochondrion (M) illustrates the typical elongated profile and the details of the tubular cristae. An oblique tangential section through the peripheral alveolar membranes of the cell exhibits the somewhat electron dense organic deposit (arrow) surrounded on both sides by the less dense alveolar membranes that appear somewhat sheet-like due to the glancing plane of the ultrathin section. Scale bar = 0.1 μm . (E and F) Profiles of chloroplasts are shown in an oblique cross section (E), exhibiting the lenticular pyrenoid (Py), and in longitudinal section (F) more clearly showing the organization of the lamellae. A cytoplasmic lobe containing a mitochondrion (M) is shown nearby to a plastid. Scale bars = 1.0 μm . (G) A high-resolution image shows the plastid fine structure containing up to three thylakoids per lamella (arrow). Scale bar = 0.1 μm .

detail. An oblique tangential section, passing through the nearby alveolar membrane complex at the periphery of the cell, shows the texture of the internal dense organic deposit (arrow) and the less dense enclosing membranes on either side. Since this is an oblique tangential section, the image displays the membranes and internal organic deposit in a partial sheet-like perspective. The chloroplasts (Fig. 5E and F) are surrounded by three membranes and contain a simple pyrenoid (Py), without

internal thylakoids. There are occasional osmiophilic granules (60 nm diameter) within the stroma of the plastid as seen more clearly at the base of the chloroplast section in Fig. 5F. A portion of an elongated mitochondrion (M) is also visible within a cytoplasmic lobe near the plastid. Each chloroplast lamella (~ 40 nm thick and 60 nm apart), shown in high magnification (Fig. 5G), contains up to three thylakoids (arrow) and is suspended in a somewhat finely granular stroma.

Our sequencing of LSU rDNA from two separate isolates from Flanders Bay, NY, USA (CpFB-06-1, CpFB-06-2), showed identical sequences among the isolates for both the D1–D3 and D4–D6 regions (GenBank accession nos. EF110556 and EF110557, respectively). The D1–D3 region sequence of NY isolates showed similarity to three GenBank sequences from Korean isolates of *C. polykrikoides* (GenBank accession nos. AY347309, AY725423, AF067861) with identities of 90, 90 and 88%, respectively. The D4–D6 region of our strains showed 89% identity with the Korean strain (AY347309). The sequencing efforts of Iwataki et al. (2008) permit our isolates to be compared to additional clones in North American and southeast Asia. The D1–D3 and D4–D6 region sequences of our isolates displayed 100% identity with two North American *C. polykrikoides* strains: CPCB10 isolated from Cotuit Bay, MA, USA, and CPPV-1, isolated from Bahia de La Paz, Mexico. Regarding the Korean and Hong Kong strains of Mikulski and Doucette (this issue; Genbank accession nos. pending), we had 90.4% alignment with their Korean and Hong Kong strains for the D1–D3 region and 97.5% alignment with the D4–D6 region. Therefore, it is clear our isolates are not con-specific with the isolates from Korea and Hong Kong identified as *C. polykrikoides*.

3.3. Bioassay experiments—shellfish

During the shellfish experiments, the bloom water treatment maintained mean *Cochlodinium* densities of $3.7 \pm 1.3 \times 10^4$ cells ml⁻¹ (range = 2.7 – 6.1×10^4 cells ml⁻¹), accounting for $91 \pm 5\%$ of the algal biomass. *Cochlodinium* was not detected in filtered water treatments throughout this experiment and was always $<10^2$ cells ml⁻¹ in the Great Peconic Bay water treatment. Bay scallops (*A. irradians*) and oysters (*C. virginica*) exposed to waters containing bloom concentrations of *Cochlodinium* experienced significantly increased mortality and significantly decreased growth rates (scallops only) relative to filtered bloom water, non-bloom water and filtered non-bloom water ($p < 0.001$ for all; Tukey test; Fig. 6). For scallops, filtered bloom water, non-bloom water and filtered non-bloom water treatments displayed growth rates of ~ 0.2 mm day⁻¹ and 100% survival of all individuals in all replicates during the 9-day experiment (Fig. 6A and B). In contrast, scallops exposed to bloom water grew half as fast, began to die within 48 h of exposure and experienced $67 \pm 13\%$ mortality by the end of the 9-day experiment (Fig. 6A and B). Oysters exposed to *Cochlodinium* bloom water displayed lower mortality than scallops ($16 \pm 3.3\%$; Fig. 6A), but significantly greater mortality than control treatments (Fig. 6A; $p < 0.05$; Tukey test).

Histopathological evaluation of scallop tissue revealed gill hyperplasia, as well as hemorrhaging in gills and digestive tracts (Fig. 7). Moreover, *Cochlodinium* cells, found within scallop gills, were associated with tissue inflammation (Fig. 7). By contrast, there were no signs of starvation in morbid individuals. The digestive glands of oysters displayed severe hemorrhaging and squamation, while apoptosis was observed in gill tissues (Fig. 7). Apoptosis was not observed in scallop

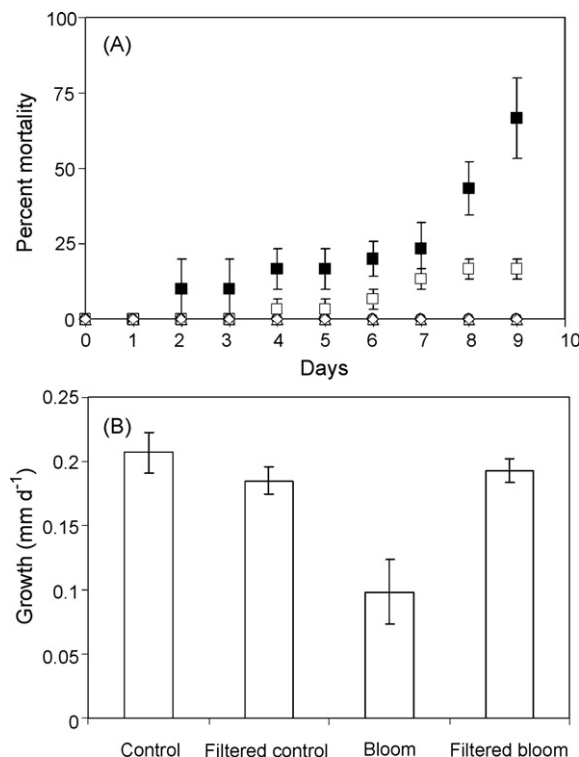


Fig. 6. Shellfish bioassay experiments. (A) Percent mortality of juvenile bay scallops (*Argopecten irradians*; closed symbols) and American oysters (*Crassostrea virginica*; open symbols) exposed to bloom water (squares), filtered (0.2 μ m) bloom water (triangles), control water from Great Peconic Bay (squares), filtered (0.2 μ m) water from Great Peconic Bay (circles). (B) Shell growth rates of juvenile bay scallops (*Argopecten irradians*) during nine exposure to the four treatments. Error bars are S.D. of triplicate containers for both graphs.

tissues. Examination of shellfish exposed to non-bloom water did not reveal any of the histopathological conditions described for the individuals exposed to bloom water.

3.4. Bioassay experiments—fish

Experiments were conducted with sheepshead minnows (*C. variegates*) using bloom water with *Cochlodinium* densities ranging from 0.6 to 1.3×10^5 cells ml⁻¹. In all experiments, controls (non-bloom water, filtered non-bloom water, and filtered bloom water) always displayed 100% survival for the duration of experiments (>72 h), demonstrating that physical contact with cells was required for fish mortality. In contrast, individuals exposed to undiluted bloom water (0.59 – 1.3×10^5 cells ml⁻¹) began to expire within 10 min, and no individual ($n = 144$) survived longer than 9 h (Fig. 8). In the most extreme experiment (*Cochlodinium* cell density = $1.3 \pm 0.2 \times 10^5$ cells ml⁻¹), fish in all 24 wells perished within 30 min. While there was no obvious relationship between the initial cell density and the survival time of minnows, there was a hyperbolic relationship between the initial cell density and the fraction of minnows surviving after 24 h (Fig. 8). Specifically, all fish survived 24 h at cell densities of $\leq 1.1 \pm 0.1 \times 10^3$ and all experiments with $>5 \times 10^4$ cells ml⁻¹ displayed 100% mortality (Fig. 8). At intermediate densities, which represented

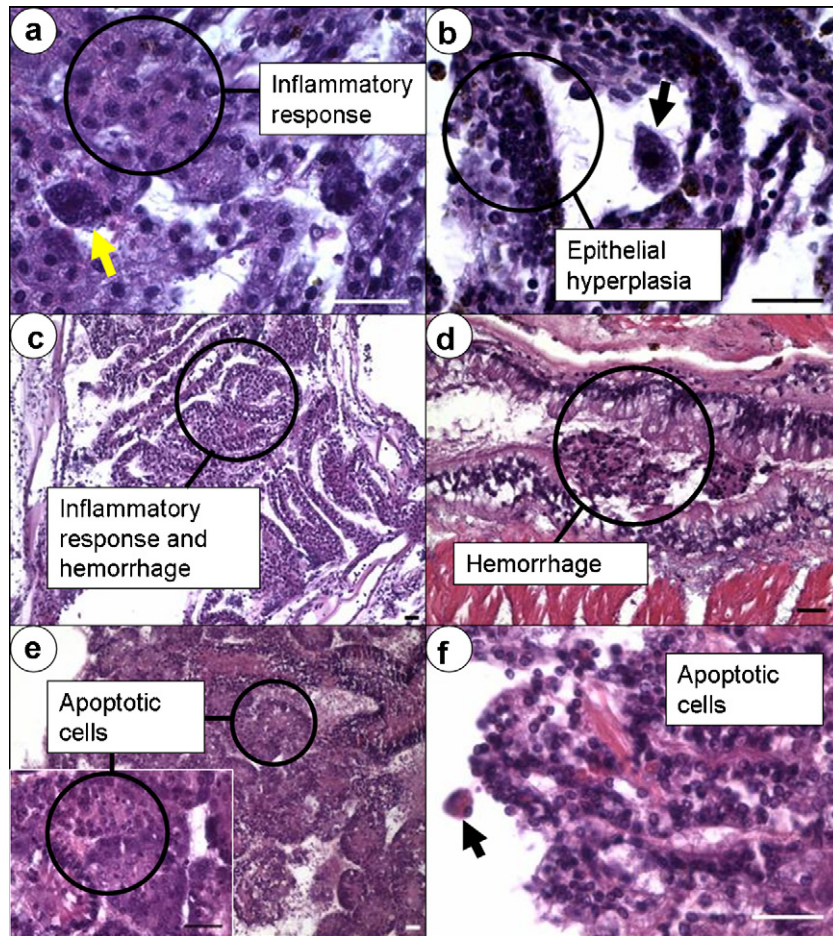


Fig. 7. Photomicrographs showing histopathological alterations in bay scallops (*Argopecten irradians*; a–d) and American oysters (*Crassostrea virginica*; e and f). (a–c) The presence of dinoflagellate-like cells in gills was associated with a severe inflammatory response and epithelial hyperplasia. Hemorrhage was also identified as free hemocytes in gill water tubules (c) and in the gut (d). In oysters, the inflammatory response in digestive gland (e) and gills (f) was associated with apoptotic figures (seen here as condensed chromatin in nucleus or round cells). Scale bar = 20 μm.

dilutions of bloom water with 0.2 μm-filtered water, the percentages of fish populations which died (4–83%) were proportional to *Cochlodinium* cell densities ($0.3\text{--}3.2 \times 10^4 \text{ ml}^{-1}$; Fig. 8). The filtration of water through a 0.2 and 2.0 μm filters resulted in 100% survival of fish for the

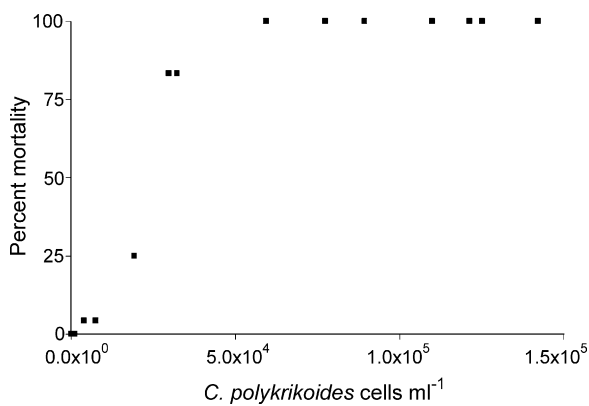


Fig. 8. *Cyprinodon variegates* bioassay experiments. Percent mortality of *Cyprinodon variegates* in 24-well plates after 24 h exposure to *Cochlodinium* bloom water containing cell densities ranging from 0 to 1.3×10^5 cells ml⁻¹.

duration of experiments, whereas mortality of fish in 10 and 20 μm filtrations were proportional to the densities of *Cochlodinium* which passed through these filters (Fig. 8). Minnows exposed to boiled or frozen cells at concentrations of $1.3 \pm 0.4 \times 10^5$ cells ml⁻¹ displayed 24 h-survival rates of 83 and 96%, respectively, which were significantly higher than that observed in the unamended bloom water (0% survival).

In the assays exposing *F. heteroclitus* to the bloom water with $9.1 \pm 0.3 \times 10^4$ cells ml⁻¹ of *Cochlodinium* (representing $94 \pm 5\%$ of the total algal biomass), the fish displayed increased mortality with time: two-thirds of individuals died within the first 4 h of exposure and $83 \pm 10\%$ expired within 24 h, in contrast to 100% survival in the control using filtered bloom water (Fig. 9A). In the experiment with *F. majalis*, the *Cochlodinium* cell densities were $9.2 \pm 0.4 \times 10^4$, $2.8 \pm 0.4 \times 10^4$, $7.2 \pm 1.1 \times 10^3$, and 0 (control) cells ml⁻¹. In the first three treatments, *Cochlodinium* accounted for >90% of the total algal biomass. Fish exposed to the highest *Cochlodinium* density experienced 100% mortality after 15 h (Fig. 9B), whereas the fish exposed to bloom water with lower cell densities ($2.8 \pm 0.4 \times 10^4$ and $7.2 \pm 1.1 \times 10^3$ cells ml⁻¹) displayed significantly lower mortality (50 ± 9.6 and $22 \pm$

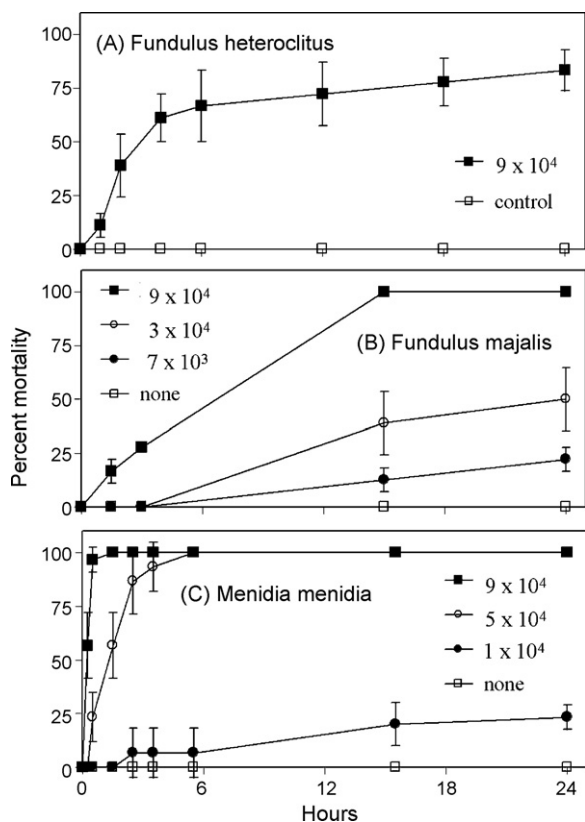


Fig. 9. Percent mortality of (A) *Fundulus heteroclitus*, (B) *Fundulus majalis*, and (C) *Menidia menidia* during 24 h exposure to varying densities of *Cochlo-dinium* bloom water. Error bars are S.D. of triplicate containers.

5.5%; Fig. 9B; $p < 0.05$; Tukey test). Fish in the filtered seawater control exhibited a 100% survival (Fig. 9B).

During the experiment with *M. menidia*, the bloom water treatments were $8.5 \pm 1.5 \times 10^4$, $4.7 \pm 1.1 \times 10^4$, and $1.3 \pm 0.2 \times 10^4$ and 0 *Cochlo-dinium* cells ml⁻¹. In the first three treatments, *Cochlo-dinium* accounted for >90% of the algal biomass. *M. menidia* exposed to *Cochlo-dinium* densities of $8.5 \pm 1.5 \times 10^4$ and $4.7 \pm 1.1 \times 10^4$ cells ml⁻¹ experienced 100% mortality after 1.5 and 5.5 h, respectively (Fig. 9C),

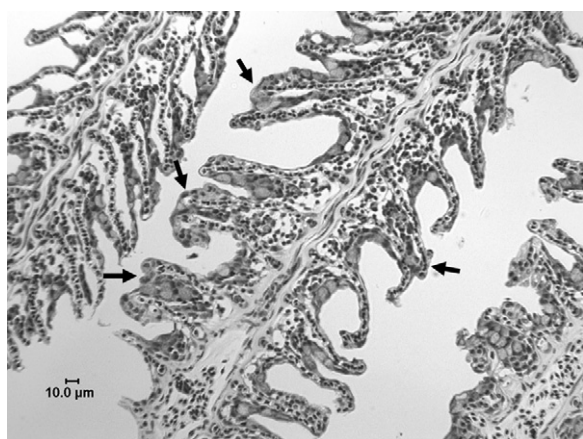


Fig. 10. Histopathological analysis of *Fundulus heteroclitus* gill tissue following 24 h exposure to *Cochlo-dinium* bloom water. Arrows depict regions of fused gill lamellae.

whereas individuals exposed to $1.3 \pm 0.2 \times 10^4$ cells ml⁻¹ displayed $23 \pm 5.7\%$ mortality during this 24 h experiment (Fig. 9C). By contrast, fish in the filtered seawater control treatment exhibited a survival rate (100%) which was significantly greater than all other treatments (Fig. 9C; $p < 0.05$; Tukey test).

The impact of *Cochlo-dinium* exposure on fish was clearly shown via histopathological examination of gill tissue. Microscopic evaluation of the gills of moribund fish demonstrated the presence of mild to moderate multifocal to diffuse epithelial proliferation (Fig. 10). Focal areas of fusion of adjacent lamellae were common (Fig. 10). Histopathological examination of the gills of fish exposed to control, non-bloom water displayed no signs of epithelial hyperplasia or fusion of adjacent lamellae.

4. Discussion

4.1. Species identification

There are multiple features of the *Cochlo-dinium* species blooming on eastern LI which are consistent with the description of *C. polykrikoides* (Margalef, 1961; Taylor et al., 1995): the cells often formed short chains consisting of two, four, and rarely eight cells; the individual cells possessed a rounded epicone; a cingulum making about two turns around the cell; slightly or heavily bilobed at the antapex (Fig. 3); a sulcus with a torsion of about one turn (Fig. 3); a red stigma located on the dorsal side of the epicone (Fig. 3); numerous band-shaped chloroplasts evenly distributed in the cell (Figs. 3 and 5F); and the nucleus is located in the epicone (Fig. 4A). As seen in *C. heterolobatum* (Silva, 1967), a synonym of *C. polykrikoides* (Taylor et al., 1995; Steidinger and Tangen, 1997), our cells also displayed a pellicle or organic envelope and two kinds of ejectosomes (an elongate trichocyst and a mucocyst; Fig. 4). Another feature of our species consistent with *C. polykrikoides* is its acute toxicity to shellfish and finfish (see Section 4.3 below). Although the presence and shape of an apical groove is unknown in our isolates at the moment, the above-listed overwhelming similarities encourage us to identify our species as *C. polykrikoides*.

Our designation of the New York bloom-forming *Cochlo-dinium* to the species *C. polykrikoides* is also strongly supported by our LSU rDNA sequences. The New York isolates showed 100% similarity with the *C. polykrikoides* isolate from Massachusetts Bay and 99.9% with the La Paz, Mexico clone in the D1–D3 region. By contrast, there were substantial differences in sequence alignment to strains from Korea and Hong Kong, with similarities ranging from 89 to 90% in this region of the LSU. Such differences, coupled with some outstanding morphological differences (e.g. cell compression) may require the designation of a new species for either the North American *Cochlo-dinium* isolates or the Korea and Hong Kong isolates in the future (Iwataki et al., 2008). Considering *C. polykrikoides* (and *C. heterolobatum* as well) was originally described from the North America, it seems it is

more reasonable to create a new species for the Asian isolates having been identified as *C. polykrikoides*.

4.2. Bloom dynamics

This study represents the first report of red tide dinoflagellate blooms caused by *C. polykrikoides* within the Peconic and Shinnecock Estuaries of eastern Long Island. While blooms caused by *C. polykrikoides* have been common in some parts of Asia, Korea and Japan in particular (Yuki and Yoshimatsu, 1989; Kim, 1998; Kim et al., 1999; Park et al., 2001; Yamatogi et al., 2006), blooms have been rarely reported in the US. Prior to this special issue, the only noted occurrence of *C. polykrikoides* blooms in the US have been in the York River, VA, and Barnegat Bay, NJ (Silva, 1967; Ho and Zubkoff, 1979). Temperatures during the bloom initiation and peak period on eastern Long Island were within the range at which *C. polykrikoides* grows optimally (21 and 26 °C), although the decline in temperature during late August and September from 25 °C to below 20 °C may have contributed to the bloom's demise (Table 1; Kim et al., 2004; Yamatogi et al., 2006). The salinities found during this study (22–30; Table 1) were generally below the optimal range for this species in Asian waters (30 and 36; Table 1; Kim et al., 2004; Yamatogi et al., 2006), perhaps evidencing an ecological difference between Asian and North American strains of *C. polykrikoides*.

Interestingly, the regions which are currently plagued with *C. polykrikoides* blooms in Long Island (Fig. 1) and Rhode Island (Tomas and Smayda, 2008) formerly hosted brown tides caused by *A. anophagefferens* during the late 1980s and 1990s (Gobler et al., 2005). In a manner similar to brown tides, *C. polykrikoides* blooms have been most intense in the far western regions of the Peconic Estuary (Flanders, Great Peconic; Fig. 1) which have the highest ambient nitrogen concentrations and the longest residence times within this system (Hardy, 1976; Nuzzi and Waters, 2004). Chlorophyll levels during the peak of *C. polykrikoides* blooms often exceeded 100 µg l⁻¹ which is five-times greater than biomass levels recorded during *Aureococcus* blooms (Gobler et al., 2005). It is likely that the higher biomass of these blooms requires a larger nutrient supply for blooms to be maintained. Unlike *Aureococcus* blooms, which achieved maximal cell densities within the major basins of the Peconic Estuary and displayed lower concentrations within creeks and tributaries, *C. polykrikoides* densities drop precipitously east of Great Peconic Bay, but are often maximal within shallow tributaries, which have high nitrogen loads (Fig. 1; Nuzzi and Waters, 2004). The stronger association of *C. polykrikoides* with regions having high levels of nitrogen suggests that it may be more directly linked with inorganic nutrient eutrophication than *Aureococcus*, which exploited estuarine regions with copious supplies of dissolved organic nitrogen but lower levels of dissolved inorganic nitrogen (LaRoche et al., 1997; Gobler and Sañudo-Wilhelmy, 2001; Gobler et al., 2005). The timing of *C. polykrikoides* blooms, which emerge during late summer (August–September), also differs from that of *Aureococcus* blooms, which typically developed during early summer (May, June; Gobler et al., 2005). Since *C. polykrikoides* has well-

documented phagotrophic capabilities (Larsen and Sournia, 1991; Jeong et al., 2004) and since blooms have been most prevalent in the regions of the Peconic estuary where nitrogen and chlorophyll *a* are highest (Nuzzi and Waters, 2004), initiation of the *C. polykrikoides* blooms may be promoted by peaks in smaller prey phytoplankton that appear during August. August previously represented the annual peak in chlorophyll *a* in the Peconic Estuary (Bruno et al., 1983).

C. polykrikoides blooms on eastern Long Island have been heterogeneous in space and time. Our sampling of both fixed stations and specific bloom 'patches' within regions of the Peconic Estuary revealed that ambient concentrations can differ by two orders of magnitude between patches and ambient water (Fig. 2). Consistent with prior research (Park et al., 2001), our preliminary observations also indicate a strong vertical component to these blooms, with 'patches' appearing in surface water during the late morning and persisting until the evening. We have also noted cells within bloom patch water can sometimes aggregate, sink, and die after a short period of containment (~2 h). As such, recording precise cell densities during *C. polykrikoides* blooms is challenging. Regardless, our rapid processing of samples in 2006 (<2 h) demonstrated that bloom patches, which can cover up to 1 km² and occupied most of the western Peconic Estuary and eastern Shinnecock Bay during late August of 2006, achieved cell densities >10⁵ cells ml⁻¹, a density consistent with prior reports of blooms by this species in North America (Whyte et al., 2001), but lower than levels reported by others in southeast Asia (Yuki and Yoshimatsu, 1989). Due to the heterogeneous nature of *C. polykrikoides* events, it seems likely that fish and shellfish would be exposed to both high (>10⁵ cells ml⁻¹) and lower concentrations of cells (~10⁴ cells ml⁻¹) during blooms.

4.3. Bloom impacts

To date, multiple investigators have reported on fish mortalities associated with *C. polykrikoides* blooms around the world (Yuki and Yoshimatsu, 1989; Whyte et al., 2001; Gárrate-Lizárraga et al., 2004). Our experimental work demonstrates the very rapid death (<24 h) of four species of fish (*C. variegates*, *F. heteroclitus*, *M. menidia*, *F. majalis*) when exposed to dense *C. polykrikoides* blooms (Figs. 8 and 9). No individual from any species survived 24 h of exposure to 10⁵ cells ml⁻¹, whereas intermediate levels of mortality occurred when experimental densities ranged from 10³ to 10⁴ cells ml⁻¹ (Figs. 8 and 9). These results are consistent with prior research conducted with salmon smolts (*Salmo salar*) and juvenile slipmouths (*Leiognathus nuchalis*) which displayed 20–90% mortality when exposed to *C. polykrikoides* cell densities ranging from 10³ to 10⁴ cells ml⁻¹ (Onoue et al., 1985; Yuki and Yoshimatsu, 1989; Whyte et al., 2001).

To date, there has been substantial controversy surrounding the mechanism of fish mortality associated with *C. polykrikoides*. While Kim et al. (1999, 2000) indicated fish mortality was associated with reactive oxygen species made by the alga, Kim et al. (2002) suggested polysaccharides were more likely to be the cause of fish mortality. To complicate

matters further, three toxic fractions (neurotoxic, hemolytic, and hemagglutinative) and two paralytic shellfish poisons (a zinc complex of carbomoyl-*N*-sulfo-11 α -hydroxyneosaxitoxin sulfate (Ic-1) and its 11 β epimer (epi-Ic-1) have been isolated from *Cochlodinium* sp. (as *Cochlodinium* type '78 Yatushiro; Onoue and Nozawa, 1989a,b). Consistent with prior findings, our experimental results demonstrate that physical contact with cells is required for fish mortality (Onoue et al., 1985; Yuki and Yoshimatsu, 1989), as all fish exposed to 0.2 or 2 μm filtered seawater survived during all experiments. Exposure of fish to cells which had been killed via freezing yielded almost no mortality (4%) in fish after 72 h while parallel whole water treatments killed all fish ($n = 24$) within 30 minutes. Our SEM and TEM micrographs revealed the presence of a thick polysaccharide coat ($>1 \mu\text{m}$) surrounding *C. polykrikoides* cells (e.g. Fig. 5), indicating this biochemical matrix may be the source of fish mortality as had been reported for this species (Kim et al., 2002) and other HABs (Gainey and Shumway, 1990). The three-dimensional structure of polysaccharides collapses upon freezing due to the loss of water and this structure is not recovered when thawed (Doerr et al., 2000; Schwarzenbach et al., 2003). Hence, the loss of ichthyotoxicity of cells upon freezing and thawing could be due to the degradation of polysaccharides, suggesting this matrix, or a principle within this matrix, is the ichthyotoxic agent associated with *C. polykrikoides*.

Fish exposed to bloom levels of *C. polykrikoides* for <48 h displayed fusion of adjacent gill lamellae (Fig. 10). The lesions observed were characteristic of an external insult to the gills which is commonly seen in external parasitic infestations, particularly in protozoal infestations (Roberts, 2001). These hyperplastic lesions suggest severe impairment of gill function (e.g. respiration, nitrogen excretion, ion balance) which could cause fish death (Roberts, 2001)

C. polykrikoides blooms on eastern Long Island may have negative impacts on ambient fish populations and, in turn, the entire ecosystem. While ambient densities of *C. polykrikoides* densities were $\sim 10^3$ cells ml^{-1} at our primary sampling sites during June and July of 2006, densities were consistently $>10^3$ cells ml^{-1} and frequently $>10^4$ cells ml^{-1} during the end of August and beginning of September of 2006. Although only sporadic fish kills were observed within tributaries during this time period, complete mortality of fish held in flow through seawater chambers at the Stony Brook-Southampton Marine Science Center was observed on multiple occasions at this time. This finding suggests that the combination of high cell densities and captivity of fish may cause maximal mortality (Whyte et al., 2001). Moreover, since most of the fish species examined during this study are important prey items for commercially important finfish in the region (Juanes et al., 1993; Juanes and Conover, 1995), *C. polykrikoides* blooms may impact the entire food web.

Previous studies have reported on the negative effects of *C. polykrikoides* on shellfish. The metamorphosis of oyster (*Crassostrea gigas*) larvae is slowed during blooms (Matsuyama et al., 2001), and mortality of larvae of the American oyster, *C. virginica*, is elevated by exposure to *C. polykrikoides*

(Ho and Zubkoff, 1979). To our knowledge, this study represents the first report of mortality in juvenile-stage *A. irradians* and *C. virginica* and reduced growth rates in *A. irradians* caused by exposure to bloom densities of *C. polykrikoides* (Fig. 6).

Histopathological evaluation of shellfish exposed to *C. polykrikoides* for approximately 1 week revealed the severe hyperplasia and gill inflammation associated with exposure to cells would cause a reduction of gas exchange within scallops (Fig. 7). Moreover, hemorrhaging and squamation of gill and digestive epithelia (Fig. 7) would leave scallops vulnerable to secondary bacterial infections which were occasionally observed in analyzed specimen (data not shown). Although these symptoms clearly indicate a deleterious effect of *C. polykrikoides* on bivalves, they are not specific enough to allow a precise mechanistic determination of the cause. We did note that scallops exposed to bloom waters were often closed, while control individuals were open and presumably feeding. Such differences were not discernable among oysters. Regardless, the presence of *C. polykrikoides* cells does elicit an inflammatory response in shellfish tissue (Fig. 7), which might be related to the polysaccharide coating of microalgal cells. It is noteworthy that Sogawa et al. (1998a,b) have demonstrated that extracellular polysaccharides produced by another dinoflagellate, *Gymnodinium* sp., are capable of inducing apoptosis in human lymphoid cells. On the other hand, prior reports documented the production by *Cochlodinium* of hemolytic toxins (Landsberg, 2002). Such toxins are capable of causing lesions and alterations in epithelial barriers of vertebrates and invertebrates similar to those observed here in gills and digestive epithelia of exposed shellfish (Landsberg, 2002).

Our results demonstrate that *C. polykrikoides* blooms may endanger native shellfish populations on eastern Long Island. During the 2005 *C. polykrikoides* bloom, a massive soft shell clam (*Mya arenaria*) mortality event occurred in Flanders Bay, when dead individuals washed up in racks on the shore line and moribund individuals were found with dinoflagellate cells in their hemorrhaged digestive tracts (B. Allam, unpublished). Bay scallops on eastern Long Island were formerly the top scallop fishery on the east coast of the US (Hoagland et al., 2002). During the intense brown tide caused by *Aureococcus* during the 1980s, the population experienced recruitment failure and a subsequent tremendous population reduction (Gobler et al., 2005). A major brown tide has not occurred in the Peconic Estuary in nearly a decade, but the scallop population has not recovered, despite ongoing efforts to reseed and restore it. Our results demonstrate that the failure of this population to recover could be due, in part, to the recent outbreaks of *C. polykrikoides* blooms in this system.

Acknowledgements

We acknowledge support from the Suffolk County Department of Health Services, Office of Ecology. We are thankful for the assistance and cooperation of the Stony Brook-Southampton Marine Science Center staff. We thank Greg Doucette and Tina Mikulski for providing LSU rDNA PCR primers and

for assistance with sequence analysis. This is contribution number 7129 from Lamont-Doherty Earth Observatory and 1350 from SoMAS.[SES]

References

- Bruno, S.F., Staker, R.D., Sharma, G.M., Turner, J.T., 1983. Primary productivity and phytoplankton size fraction dominance in a temperate North Atlantic estuary. *Estuaries* 6, 200–211.
- Coyne, K.J., Hutchins, D.A., Hare, C.E., Cary, S.C., 2001. Assessing temporal and spatial variability in *Pfiesteria piscicida* distributions using molecular probing techniques. *Aquat. Microb. Ecol.* 24, 275–285.
- Dempster, E.L., Pryor, K.V., Francis, D., Young, J.E., Rogers, H.J., 1999. Rapid DNA extraction from ferns for PCR-based analyses. *Biotechniques* 27, 66–68.
- Doerr, S.H., Shakesby, R.A., Walsh, R.P.D., 2000. Soil water repellency: its causes, characteristics and hydro-geomorphological significance. *Earth Sci. Rev.* 51, 33–65.
- Gainey, L.F., Shumway, S.E., 1990. The physiological effect of *Aureococcus anophagefferens* (“brown tide”) on the lateral cilia of bivalve mollusks. *Biol. Bull.* 181, 298–306.
- Gárrate-Lizárraga, I., Lopez-Cortes, D.J., Bustillis-Guzmán, J.J., Hernandez-Sandoval, R., 2004. Blooms of *Cochlodinium polykrikoides* (Gymnodiniaceae) in the Gulf of California, Mexico. *Rev. Biol. Trop.* 52, 51–58.
- Gobler, C.J., Sañudo-Wilhelmy, S.A., 2001. Temporal variability of groundwater seepage and brown tide blooms in a Long Island embayment. *Mar. Ecol. Prog. Ser.* 217, 299–309.
- Gobler, C.J., Renaghan, M.J., Buck, N.J., 2002. Impacts of nutrients and grazing mortality on the abundance of *Aureococcus anophagefferens* during a New York brown tide bloom. *Limnol. Oceanogr.* 47, 129–141.
- Gobler, C.J., Lonsdale, D.J., Boyer, G.L., 2005. A synthesis and review of causes and impact of harmful brown tide blooms caused by the alga, *Aureococcus anophagefferens*. *Estuaries* 28, 726–749.
- Guzmán, H.M., Cortes, J., Glynn, P.W., Richmond, R.H., 1990. Coral mortality associated with dinoflagellate blooms in the eastern Pacific (Costa Rica and Panama). *Mar. Ecol. Prog. Ser.* 60, 299–303.
- Hardy, C.D., 1976. A Preliminary Description of the Peconic Bay Estuary. Marine Sciences Research Center, State University of New York at Stony Brook. Special Report 3.
- Hasle, G.R., 1978. Settling: the inverted-microscope method. In: Sournia, A. (Ed.), *Phytoplankton Manual*. UNESCO, Paris, pp. 88–96.
- Ho, M.-S., Zubkoff, P.L., 1979. The effects of a *Cochlodinium heterolobatum* bloom on the survival and calcium uptake by larvae of the American oyster, *Crassostrea virginica*. In: Taylor, D.L., Seliger, H.H. (Eds.), *Toxic Dinoflagellate Blooms*. Elsevier, New York, pp. 409–412.
- Hoagland, P., Anderson, D.M., Kaoru, Y., White, A.W., 2002. The economic effects of harmful algal blooms in the United States: estimates, assessment issues and informational needs. *Estuaries* 25, 819–837.
- Iwataki, M., Kawami, H., Mizushima, K., Mikulski, C.M., Doucette, G.J., Relox, J.R., Anton, A., Fukuyo, Y., Matsuoka, K., 2008. Phylogenetic relationships in the harmful dinoflagellate *Cochlodinium polykrikoides* (Gymnodiniales Dinophyceae) inferred from LSU rDNA sequences. *Harmful Algae* 7, 271–277.
- Jeong, H.J., Yoo, Y.D., Kim, J.S., Kim, T.H., Kim, J.H., Kang, N.S., Yih, W., 2004. Mixotrophy in the phototrophic harmful alga *Cochlodinium polykrikoides* (dinophycean): prey species, the effects of prey concentration, and grazing impact. *J. Euk. Microbiol.* 51, 563–569.
- Juanes, F., Marks, R.E., McKown, K.A., Conover, D.O., 1993. Predation by age-0 bluefish on age-0 anadromous fishes in the Hudson River estuary. *Trans. Am. Fish. Soc.* 122, 348–356.
- Juanes, F., Conover, D.O., 1995. Size-structured piscivory: advection and linkage between predator and prey recruitment in young-of-the-year bluefish. *Mar. Ecol. Prog. Ser.* 128, 287–304.
- Kim, H.G., 1998. *Cochlodinium polykrikoides* blooms in Korean coastal waters and their mitigation. In: Reguera, B., Blanco, J., Fernandez, M.L., Wyatt, T. (Eds.), *Harmful Algae*. Xunta de Galicia and Intergovernmental Oceanographic Commission of UNESCO, Spain, pp. 227–228.
- Kim, C.S., Lee, S.G., Kim, H.G., Jung, J., 1999. Reactive oxygen species as causative agents in the ichthyotoxicity of the red tide dinoflagellate *Cochlodinium polykrikoides*. *J. Plankton Res.* 21, 2105–2115.
- Kim, C.S., Lee, S.G., Kim, H.G., 2000. Biochemical responses of fish exposed to a harmful dinoflagellate *Cochlodinium polykrikoides*. *J. Expt. Mar. Biol. Ecol.* 254, 131–141.
- Kim, D., Oda, T., Muramatsu, T., Kim, D., Matsuyama, Y., Honjo, T., 2002. Possible factors responsible for the toxicity of *Cochlodinium polykrikoides*, a red tide phytoplankton. *Comp. Biochem. Physiol. C—Toxicol. Pharmacol.* 132, 415–423.
- Kim, D.I., Matsuyama, Y., Nagasoe, S., Yamaguchi, M., Yoon, Y.H., Oshima, Y., Imada, N., Honjo, T., 2004. Effects of temperature, salinity and irradiance on the growth of the harmful red tide dinoflagellate *Cochlodinium polykrikoides* Margalef (Dinophyceae). *J. Plankton Res.* 26, 61–66.
- LaRoche, J., Nuzzi, R., Waters, R., Wyman, K., Falkowski, P.G., Wallace, D.W.R., 1997. Brown tide blooms in Long Island’s coastal waters linked to interannual variability in groundwater flow. *Global Change Biol.* 3, 397–410.
- Larsen, J., Sournia, A., 1991. Diversity of heterotrophic dinoflagellates. In: Patterson, D.J., Larsen, J. (Eds.), *The Biology of Free-living Heterotrophic Dinoflagellates*. Clarendon Press, Oxford, pp. 313–332.
- Landsberg, J.H., 2002. The effects of harmful algal blooms on aquatic organisms. *Rev. Fisheries Sci.* 10, 113–390.
- Luna, L.G., 1968. *Manual of Histologic Staining Methods of the Armed Forces Institute of Pathology*, third ed. McGraw-Hill, New York.
- Margalef, R., 1961. Hidrografia y fitoplancton de un área marina de la costa meridional de Puerto Rico. *Invest. Pesqui.* 18, 33–96.
- Matsuyama, Y., Usuki, H., Uchida, T., Kotani, Y., 2001. Effects of harmful algae on the early planktonic larvae of the oyster *Crassostrea gigas*. In: Hallegraeff, G.M., Blackburn, S.I., Bolch, C.J., Lewis, R.J. (Eds.), *Proceedings of the Ninth International Conference on Harmful Algal Blooms*, IOC of UNESCO, Paris, pp. 411–414.
- Mikulski, C.M., Morton, S.L., Doucette, G.J., 2005. Development and application of LSU rRNA probes for *Karenia brevis* in the Gulf of Mexico, USA. *Harmful Algae* 4, 49–60.
- Nuzzi, R., Waters, R.M., 2004. Long-term perspective on the dynamics of brown tide blooms in Long Island coastal bays. *Harmful Algae* 3, 279–293.
- Okaichi, T., 2003. *Red Tides*. Terra Scientific Publishing Company, Tokyo, 439 pp.
- Onoue, Y., Nozawa, K., Kumanda, K., Takeda, K., Aramaki, T., 1985. Toxicity of *Cochlodinium* ’78 Yatsushiro occurring in Yatsushiro Sea. *Nippon Suisan Gakkaishi* 51, 147–151.
- Onoue, Y., Nozawa, K., 1989a. Separation of toxins from harmful red tides occurring along the coast of Kagoshima Prefecture. In: Okaichi, T., Anderson, D.M., Nemoto, T. (Eds.), *Red Tides, Biology, Environmental Science and Toxicology*. Elsevier, New York, pp. 371–374.
- Onoue, Y., Nozawa, K., 1989b. Zinc-bound PSP toxins separated from *Cochlodinium* red tide. In: Natori, S., Hashimoto, K., Ueno, Y. (Eds.), *Mycotoxins and Phycotoxins* ’88. Elsevier, Amsterdam, pp. 359–366.
- Park, J.G., Jeong, M.K., Lee, J.A., Cho, K.J., Kwon, O.S., 2001. Diurnal vertical migration of a harmful dinoflagellate, *Cochlodinium polykrikoides* (Dinophyceae), during a red tide in coastal waters of Namhae Island, Korea. *Phycologia* 40, 292–297.
- Parsons, T.R., Maita, Y., Lalli, C.M., 1984. *A Manual of Chemical and Biological Methods for Seawater Analysis*. Pergamon Press, Oxford.
- Qi, D., Huang, Y., Wang, X., 1993. Toxic dinoflagellate red tide by a *Cochlodinium* sp. along the coast of Fujian, China. In: Smayda, T.J., Shimizu, Y. (Eds.), *Toxic Phytoplankton Blooms in the Sea*. Elsevier, Amsterdam, pp. 235–238.
- Roberts, R.J., 2001. *Fish Pathology*, third ed. W.B. Saunders, New York, 472 pp.
- Ryther, J.H., 1954. The ecology of phytoplankton blooms in Moriches Bay and Great South Bay. *Biol. Bull.* 106, 198–206.
- Ryther, J.H., 1989. Historical perspective of phytoplankton blooms on Long Island and the Green Tides of the 1950’s. In: Cosper, E.M., Bricelj, V.M., Carpenter, E.J. (Eds.), *Novel Phytoplankton Blooms: Causes and Impacts of Recurrent Brown Tides and Other Unusual Blooms*. Springer, New York, pp. 375–382.
- Schwarzenbach, R.P., Gschwend, P.M., Imboden, D.M., 2003. *Environmental Organic Chemistry*. Wiley.

- Shin, K., Jang, M.C., Jang, P.K., Ju, S.J., Lee, T.K., Chang, M., 2003. Influence of food quality on egg production and viability of the marine planktonic copepod *Acartia omorii*. *Prog. Oceanogr.* 57, 265–277.
- Silva, E.S., 1967. *Cochlodinium heterolobatum* n.sp.: structure and some cytophysiological aspects. *J. Protozool.* 14, 745–754.
- Smayda, T.J., 1978. From phytoplankters to biomass. In: Sournia, A. (Ed.), *Phytoplankton Manual*. UNESCO, Paris, pp. 273–279.
- Sogawa, K., Matsuda, M., Okutani, K., 1998a. Induction of apoptosis by a marine microalgal polysaccharide in a human leukemic cell line. *J. Mar. Biotechnol.* 6, 241–243.
- Sogawa, K., Kodama, E., Matsuda, M., Shigeta, S., Okutani, K., 1998b. Marine microalgal polysaccharide induces apoptosis in human lymphoid cells. *J. Mar. Biotechnol.* 6, 35–38.
- Sokal, R.R., Rohlf, F.J., 1995. *Biometry: The Principles and Practice of Statistics in Biological Research*, third ed. W.H. Freeman and Company, New York, NY, 887 pp.
- Steidinger, K.A., Tangen, K., 1997. Dinoflagellates. In: Tomas, C.R. (Ed.), *Identifying Marine Phytoplankton*. Academic Press, London, pp. 387–589.
- Stoecker, D.K., Sieracki, M.E., Verity, P.G., Michaels, A.E., Haugen, E., Burkill, P.H., Edwards, E.S., 1994. Nanoplankton and protozoan microzooplankton during the JGOFS N Atlantic Bloom Experiment: 1989 and 1990. *J. Mar. Biol. Assoc. U.K.* 74, 427–443.
- Taylor, F.J.R., Fukuyo, Y., Larsen, J., 1995. Taxonomy of harmful dinoflagellates. In: Hallegraeff, G.M., Anderson, D.M., Cembella, A. (Eds.), *Manual on Harmful Marine Microalgae*. UNESCO, Paris, pp. 339–364.
- Tomas, C.R., Smayda, T.J., 2008. Red tide blooms of *Cochlodinium polykrioides* in a coastal cove. *Harmful Algae* 7, 308–317.
- Whyte, J.N.C.I., Haigh, N., Ginther, N.G., Keddy, L.J., 2001. First record of blooms of *Cochlodinium* sp (Gymnodiniales Dinophyceae) causing mortality to aquacultured salmon on the west coast of Canada. *Phycologia* 40, 298–304.
- Yamatogi, T., Sakaguchi, M., Iwataki, M., Matsuoka, K., 2006. Effects of temperature and salinity on the growth of four harmful red tide flagellates occurring in Isahaya Bay in Ariake Sound, Japan. *Nippon Suisan Gakkaishi* 72, 160–168.
- Yuki, K., Yoshimatsu, S., 1989. Two fish-killing species of *Cochlodinium* from Harima-Nada, Seto Inland Sea Japan. In: Okaichi, T., Anderson, D.M., Nemoto, T. (Eds.), *Red Tides: Biology, Environmental Science, and Toxicology*. Elsevier, New York, pp. 451–454.